

Thermal Hall Effect of Spin Waves in a Frustrated Kagomé Antiferromagnet

S. A. Owerre^{1,2}

¹*Perimeter Institute for Theoretical Physics, 31 Caroline St. N., Waterloo, Ontario N2L 2Y5, Canada.*

²*African Institute for Mathematical Sciences, 6 Melrose Road, Muizenberg, Cape Town 7945, South Africa.*

(Dated: December 9, 2024)

In frustrated magnets the Dzyaloshinsky-Moriya interaction (DMI) can induce a long range magnetic order. Here we show that the topological properties of magnetic spin excitations in frustrated kagomé antiferromagnets stem from field-induced noncoplanar magnetic spin texture with finite scalar spin chirality in stark contrast to collinear ferromagnets with DMI. This result applies to a wide range of frustrated kagomé magnets as the scalar spin chirality is the hallmark of many exotic properties of quantum spin liquids.

Introduction–. Topological phases of matter are active research field in condensed matter physics, mostly dominated by electronic systems. Quite recently the concepts of topological matter have been extended to nonelectronic systems such as quantized spin waves (magnons) [1–17] and quantized lattice vibrations (phonons) [18–23]. In the former, spin-orbit coupling (SOC) manifests in the form of DMI [24, 25] and it leads to topological spin excitations and chiral edge modes in collinear ferromagnets [5, 6]. The quantized spin waves or magnons are charge-neutral quasiparticles and they do not experience a Lorentz force as in charge particles. However, a temperature gradient can induce a heat current and the DMI-induced Berry curvature acts as an effective magnetic field. This leads to a thermal Hall effect characterized by a temperature dependent thermal Hall conductivity [1, 3]. Thermal Hall effect is now an emerging active research area for probing the topological nature of magnetic spin excitations in quantum magnets. The thermal Hall effect of spin waves has been realized experimentally in a number of pyrochlore ferromagnets [2, 4]. Recently, DMI-induced topological magnon bands and thermal Hall effect have been observed in collinear kagomé ferromagnet Cu(1-3, bdc) [8, 9]. These materials are believed to be useful for designing systems with less dissipation applicable to magnon spintronics.

In frustrated kagomé magnets, however, there is no magnetic long range order even at the lowest accessible temperatures. The classical ground states have an extensive degeneracy and they are considered as candidates for quantum spin liquids (QSL) [29]. However, recent experimental syntheses of materials have shown that the effects of SOC or DMI are not negligible in frustrated magnets. The DMI is an intrinsic perturbation to the Heisenberg interaction. One of the striking features of the DM perturbation is that it can induce a long range magnetic order with a $\mathbf{q} = 0$ propagation vector in frustrated kagomé magnets [30]. Hence, the DMI suppresses the quantum spin liquid phase of frustrated kagomé antiferromagnets up to a critical value [31]. The syntheses of materials have shown that various experimentally accessible frustrated kagomé antiferromagnets show evidence of noncollinear $\mathbf{q} = 0$ magnetic long range order at specific temperatures [30–36]. The famous ones are iron jarosites, specifically

the potassium iron jarosite $\text{KFe}_3(\text{OH})_6(\text{SO}_4)_2$ [30, 32]. However, the role of DMI in frustrated kagome magnets has not been investigated in the context of thermal Hall effect and topological spin excitations. Here we provide a theoretical evidence of thermal Hall effect and topological spin excitations in frustrated kagomé magnets. We show that the DMI is not the primary source of thermal Hall effect in frustrated kagomé magnets as opposed to collinear magnetic systems.

Model–. We consider the Hamiltonian for kagomé antiferromagnets given by [33, 34]

$$\mathcal{H} = \sum_{\langle i,j \rangle} \mathcal{J}_{ij} \mathbf{S}_i \cdot \mathbf{S}_j + \sum_{\langle i,j \rangle} \mathcal{D}_{ij} \cdot \mathbf{S}_i \times \mathbf{S}_j, \quad (1)$$

where \mathbf{S}_i is the spin moment at site i , $\mathcal{J}_{ij} = \mathcal{J}$, $\mathcal{J}_2 > 0$ are the isotropic antiferromagnetic couplings for nearest-neighbour (NN) and next-nearest-neighbour (NNN) sites respectively. According to Moriya rules [25], the midpoint between two magnetic ions on the kagomé lattice is not an inversion center. Therefore the DM vector \mathcal{D}_{ij} can be allowed on the kagomé lattice as shown in Fig. 1. In ferromagnets the DMI leads to topological spin waves [1–17], whereas in the present model the DMI is known to stabilize the 120° coplanar $\mathbf{q} = 0$ magnetic structure [30]. Besides, the NNN coupling $\mathcal{J}_2 > 0$ can equally stabilize the coplanar magnetic structure [37]. We will consider the out-of-plane intrinsic DMI $\mathcal{D}_{ij} = (0, 0, \mp \mathcal{D}_z)$, where $-/+$ alternates between up/down triangles of the kagomé lattice as shown in Fig. 1. There is only one ground state for each sign of the DMI [30]. The DMI breaks the global $\text{SO}(3)$ rotation symmetry of the Hamiltonian down to $\text{SO}(2)$ global spin rotation symmetry in the x - y plane. An in-plane component might be present if there is no mirror reflection symmetry on the lattice. The in-plane component breaks the global spin rotation symmetry and leads to spin canting with weak out-of-plane ferromagnetic moment. However, most kagomé antiferromagnets have very small negligible in-plane DM component due to dominant out-of-plane component [31, 34]. Therefore its presence will not change the basic results of this paper.

Dirac spin waves–. As we pointed out above, the present model differs significantly from collinear ferromagnets because the DMI does not play the same role in both systems. This is probably the reason why the topo-

logical properties of (1) have not been scrutinized. From symmetry point of view, the mirror reflection symmetry with respect to the kagomé planes is a good symmetry of the kagomé lattice. But this symmetry reverses the 120° coplanar spins, and under time-reversal symmetry the spin will return to the original states. Therefore the combination of mirror reflection and time-reversal symmetries leaves the 120° coplanar spins invariant. Figure 2 shows the spin wave excitations of the 120° coplanar spins along the high symmetry points of the Brillouin zone [39] with $\Gamma = (0, 0)$, $\mathbf{M} = (\pi/2, \pi/2\sqrt{3})$ and $\mathbf{K} = (2\pi/3, 0)$ (see Ref. [38] for detail). For $\mathcal{J}_2 \neq 0, \mathcal{D}_z \neq 0$ there is only SO(2) rotation symmetry in the x - y plane. There are two dispersive bands and one nearly flat mode corresponding to a lifted zero mode. For $\mathcal{J}_2 \neq 0, \mathcal{D}_z = 0$ the global SO(3) rotation symmetry is restored and the three dispersive bands have Goldstone modes at Γ . The interesting feature of this system is the linear band crossing of two magnon branches at \mathbf{K} , which realizes a two-dimensional (2D) Dirac Hamiltonian

$$\mathcal{H}(\pm\mathbf{K} + \mathbf{q}) = c_0 \mathbb{I}_{2 \times 2} + c_1 (\pm q_x \sigma_x + q_y \sigma_y), \quad (2)$$

where \mathbf{q} is the momentum vector, c_0 and c_1 are functions of the Hamiltonian parameters, σ is a Pauli matrix and $\mathbb{I}_{2 \times 2}$ is an identity matrix. The linearized Hamiltonian (2) has winding number ± 1 for states at $\pm\mathbf{K}$ and it is different from the Goldstone modes of continuous rotational symmetry breaking. The Dirac points are protected by a combination of mirror reflection and time-reversal symmetry. The presence of Dirac points in the presence of SOC (in this case DMI) is the basis of Weyl magnon [15, 16] and Dirac semimetal in electronic systems [40]. Thus, the present model can be regarded as a magnon analog of quasi-2D Dirac semimetal. A thorough study of Dirac magnon points with DMI is beyond the purview of this Letter and will be presented in detail elsewhere.

Topological spin waves. We expect the Dirac magnon points to be at the boundary between topological and trivial insulators just like in electronic systems. Therefore, the system can be driven to a topological phase by breaking the symmetries that protect the Dirac magnon points. As we previously mentioned, an in-plane DMI breaks mirror reflection symmetry but preserves time-reversal symmetry, thus it is capable of lifting the Dirac magnon points. However, due to a dominant out-of-plane DM component, the value of the in-plane DM component is usually suppressed in most kagomé antiferromagnetic crystals [31, 34]. Hence, the effects of in-plane DMI can be negligible and the Dirac magnon points will persist. The system can be driven to a topological phase by applying a magnetic field perpendicular to the kagomé plane given by $\mathcal{H}_Z = -\mathbf{B} \cdot \sum_i \mathbf{S}_i$, where $\mathbf{B} = g\mu_B \mathcal{B}_z \hat{\mathbf{z}}$, g is the g -factor and μ_B is the Bohr magneton. The out-of-plane Zeeman field breaks time reversal symmetry but preserves mirror reflection symmetry. In this case, however, time reversal symmetry is broken through a field-induced non-coplanar spin texture with nonzero scalar spin chirality [38] $\mathcal{H}_\chi \sim \cos \chi \sum \mathbf{S}_i \cdot (\mathbf{S}_j \times \mathbf{S}_k)$, where $\cos \chi = h/h_s$

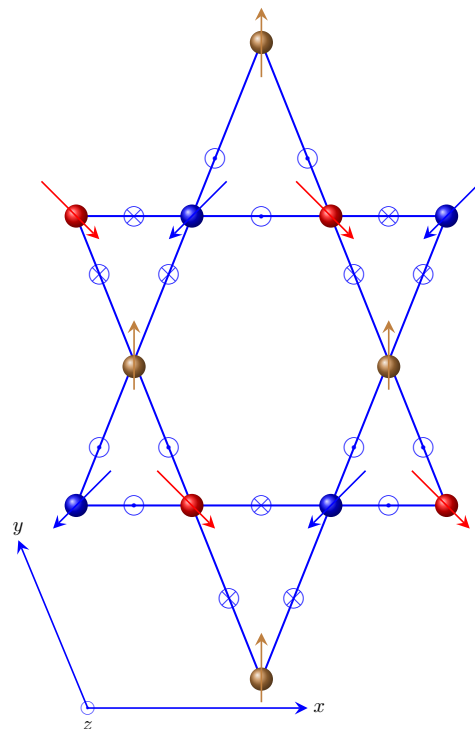


FIG. 1: Color online. Coplanar $\mathbf{q} = 0$ spin configuration on the kagomé lattice with alternating DMI at the midpoint between two magnetic ions.

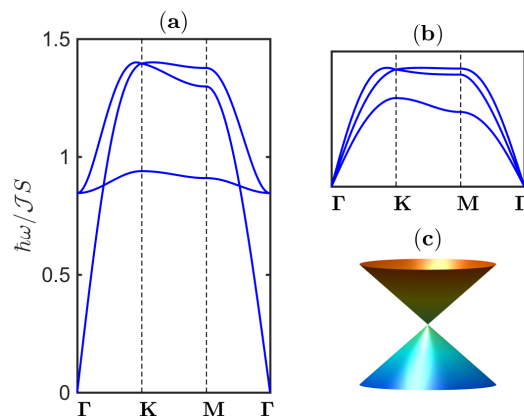


FIG. 2: Color online. Spin wave excitations of Eq. 1. (a) $\mathcal{D}/\mathcal{J} = 0.12, \mathcal{J}_2/\mathcal{J} = 0.03$. (b) $\mathcal{D}/\mathcal{J} = 0, \mathcal{J}_2/\mathcal{J} = 0.2$. (c) Gapless Dirac cone of two top bands at \mathbf{K} .

with $h_s = [6(\mathcal{J} + \mathcal{J}_2) + 2\sqrt{3}\mathcal{D}_z]$ and $h = g\mu_B \mathcal{B}_z$. The scalar chirality changes sign by 180° rotation of the spins, that is $\mathcal{H}_\chi \rightarrow -\mathcal{H}_\chi$ as $\chi \rightarrow \pi + \chi$. The propagation of magnon around a set of three non-coplanar magnetic moments gives rise to a fictitious magnetic flux ϕ and the Berry curvature is related to the solid angle subtended by the three spins on each triangular plaquette. It should be noted that in frustrated magnets scalar spin chirality is the basis of chiral QSL in which both time-reversal and

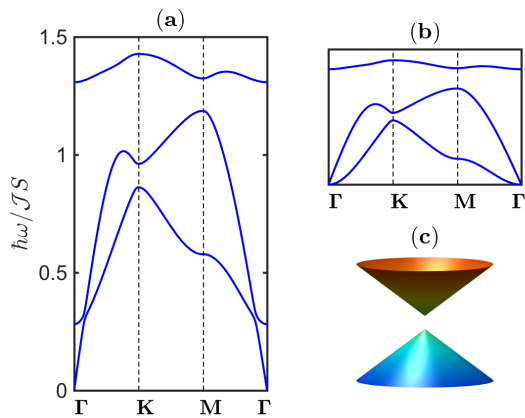


FIG. 3: Color online. Topological spin wave excitations of Eq. 1 at finite magnetic field $h/h_s = 0.4$. (a) $\mathcal{D}_z/\mathcal{J} = 0.06$, $\mathcal{J}_2/\mathcal{J} = 0.03$ and $\mathcal{J} = 3.34$ meV. This corresponds to the parameter values of $\text{KFe}_3(\text{OH})_6(\text{SO}_4)_2$ [33]. (b) $\mathcal{D}_z/\mathcal{J} = 0$. (c) Gap Dirac cone of two bands at \mathbf{K} .

parity symmetries are broken without any magnetic long range order $\langle \mathbf{S}_j \rangle = 0$. In fact, the origin of scalar spin chirality in this model is due to geometrical spin frustration and does not necessarily require the presence of DMI. This is a crucial difference between frustrated magnets and previously studied unfrustrated systems [1–17].

The magnon energy branches of the noncoplanar spin textures are shown in Fig. 3 with the parameter values of $\text{KFe}_3(\text{OH})_6(\text{SO}_4)_2$ [33] with/without DMI. The dispersions show a finite gap at all points in the Brillouin zone. The linearized Hamiltonian for two avoided band crossing at $\pm\mathbf{K}$ can be written as

$$\mathcal{H}(\pm\mathbf{K} + \mathbf{q}) = c_0 \mathbb{1}_{2 \times 2} + c_1 (\pm q_x \sigma_x + q_y \sigma_y) + m(\phi) \sigma_z, \quad (3)$$

where $m(\phi) \propto \phi$ and $\sin \phi$ is related to the scalar spin chirality. In principle, a gap Dirac point is not enough to prove that a system is topological. To further substantiate the topological nature of the system we have solved for the chiral edge modes using a strip geometry with open boundary conditions along the y direction and infinite along x direction [26] as depicted in Fig. 4. At zero magnetic field $\mathcal{H}_\chi = 0$, there are no gapless edge modes, but a single edge mode connects the Dirac points of the dispersive bands. As the magnetic field is turned on $\mathcal{H}_\chi \neq 0$, we clearly see gapless edge modes between the upper and middle bands, which signify a strong topological magnon insulator [5]. Because of the bosonic nature of magnons there is no Fermi energy or completely filled bands in this system. Nevertheless, a Chern number can still be defined for this system as shown in Ref. [38]. The Chern numbers in the topological regime are calculated as $[0, -\text{sgn}(\sin \phi), \text{sgn}(\sin \phi)]$ for the lower, middle, and upper bands respectively. This confirms that the system is in the topological regime.

Thermal Hall effect-. Having established the topologi-

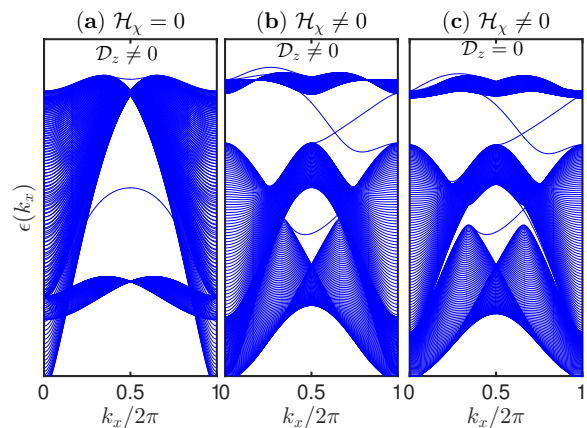


FIG. 4: Color online. Chiral spin wave edge modes for two field values $h/h_s = 0$ ($\mathcal{H}_\chi = 0$) and $h/h_s = 0.4$ ($\mathcal{H}_\chi \neq 0$) with and without DMI. The parameters are the same as Fig. 3.

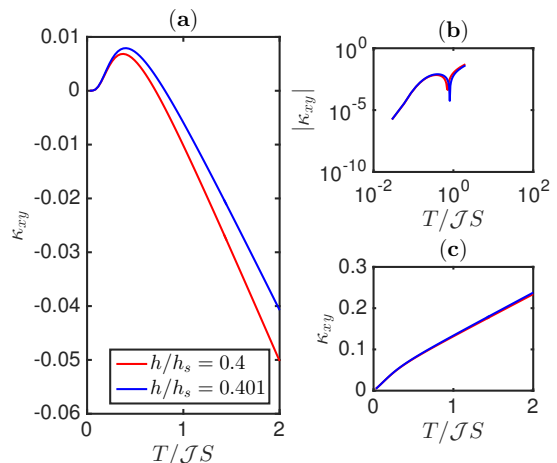


FIG. 5: Color online. Low-temperature dependence of κ_{xy} for with the parameters of $\text{KFe}_3(\text{OH})_6(\text{SO}_4)_2$ (see Fig. 3). (a) κ_{xy} vs. T . (b) Log-log plot of $|\kappa_{xy}|$ vs. T . (c) κ_{xy} vs. T without DMI.

cal nature of the system, now we will investigate another aspect of this insulator which is experimentally accessible. The measurement of thermal Hall response using inelastic neutron scattering is the new method to probe the topological nature of spin excitations in insulating quantum magnets [2, 8, 9]. In some respects, it is analogous to quantum anomalous Hall effect in electronic systems, but requires a temperature gradient and a heat current. From linear response theory, the general formula for thermal Hall conductivity of spin excitations κ_{xy} can be derived, see Ref. [7]. The low-temperature dependence of κ_{xy} for the present model is plotted in Fig. 5(a) with the parameter values of $\text{KFe}_3(\text{OH})_6(\text{SO}_4)_2$ [32]. At zero magnetic field there is no thermal Hall effect in accordance with the analysis of topological spin waves and edge modes discussed above. The log-log plot in Fig. 5(b) indicates that the low-temperature dependence of κ_{xy} is not linear.

The crucial features of this model is that for zero DMI $\mathcal{D}_{ij} = 0$, the NNN coupling $\mathcal{J}_2 > 0$ also stabilizes the $\mathbf{q} = 0$ coplanar structure as mentioned above [37] and thermal Hall effect is present as shown in Fig. 5(c). The easy-plane anisotropy in the XXZ kagomé antiferromagnet without DMI also stabilizes the $\mathbf{q} = 0$ magnetic long range order. In this case both topological spin waves and edge modes are present as detailed in Ref. [38]. This is a distinguishing feature of this model and it is crucial because the experimental determination of DMI is immaterial as it does not lead to a finite κ_{xy} in frustrated systems. These features should be important in many experimentally accessible kagomé antiferromagnets [31, 32, 34]. In particular, Fe-jarosite $\text{KFe}_3(\text{OH})_6(\text{SO}_4)_2$ [32] meets all the requirements predicted in this Letter. In frustrated electronic systems anomalous Hall response arising from scalar spin chirality is called topological Hall effect [41–45]. The present model is an analog of this effect in quantum magnets with charge-neutral magnetic spin excitations. It will be of interest to study experimentally. The main result of this Letter is that a combination of geometrical spin frustration and kagomé antiferromagnets can realize thermal Hall effect without the need of DMI or SOC.

Conclusion–. We have shown that geometrical spin

frustration on the kagomé antiferromagnets can lead to field-induced scalar spin chirality even in the absence of DMI. The field-induced scalar chirality provides topological spin excitations and thermal Hall response applicable to different frustrated kagomé magnets. These results are experimentally accessible. Besides, it will be interesting to probe magnon analogs of “Dirac semimetal” in quantum magnets as pointed out here. The chiral edge modes have not been measured at the moment and they require edge sensitive methods such as light [46] or electronic [47] scattering method. We recently became aware of a recent experimental report of thermal Hall response in frustrated distorted kagomé volborthite at a \mathcal{B} -field of 15 T with no signs of DMI [48]. However, the exact Hamiltonian for volborthite and its parameter values remain controversial. The results presented here apply specifically to undistorted kagomé antiferromagnets. In this regard, the present study will be important in upcoming experimental studies of finite thermal Hall response in frustrated kagomé magnets.

Acknowledgements–. Research at Perimeter Institute is supported by the Government of Canada through Industry Canada and by the Province of Ontario through the Ministry of Research and Innovation.

-
- [1] H. Katsura, N. Nagaosa, and P. A. Lee, Phys. Rev. Lett. **104**, 066403 (2010).
- [2] Y. Onose, T. Ideue, H. Katsura, Y. Shiomi, N. Nagaosa, Y. Tokura, Science **329**, 297 (2010).
- [3] R. Matsumoto and S. Murakami, Phys. Rev. Lett. **106**, 197202 (2011); Phys. Rev. B **84**, 184406 (2011).
- [4] T. Ideue, Y. Onose, H. Katsura, Y. Shiomi, S. Ishiwata, N. Nagaosa, and Y. Tokura, Phys. Rev. B. **85**, 134411 (2012).
- [5] Lifa Zhang, Jie Ren, Jian-Sheng Wang, and Baowen Li, Phys. Rev. B **87**, 144101 (2013).
- [6] A. Mook, J. Henk, and I. Mertig, Phys. Rev. B **90**, 024412 (2014); Phys. Rev. B **89**, 134409 (2014).
- [7] R. Matsumoto, R. Shindou, and S. Murakami, Phys. Rev. B **89**, 054420 (2014).
- [8] R. Chisnell, J. S. Helton, D. E. Freedman, D. K. Singh, R. I. Bewley, D. G. Nocera, and Y. S. Lee, Phys. Rev. Lett. **115**, 147201 (2015).
- [9] Max Hirschberger, Robin Chisnell, Young S. Lee, N. P. Ong, Phys. Rev. Lett. **115**, 106603 (2015).
- [10] H. Lee, J. H. Han, and P. A. Lee, Phys. Rev. B **91**, 125413 (2015).
- [11] D. Boldrin, B. Fak, M. Enderle, S. Bieri, J. Ollivier, S. Rols, P. Manuel, and A. S. Wills, Phys. Rev. B **91**, 220408(R) (2015).
- [12] S. A. Owerre, J. Phys.: Condens. Matter **28**, 386001 (2016).
- [13] S. A. Owerre, J. Appl. Phys. **120**, 043903 (2016).
- [14] F.-Y. Li, Y.-D. Li, Y.-B. Kim, L. Balents, Y. Yu, and G. Chen, Nat. Commun. **7**, 12691 (2016).
- [15] Mook, A., Henk, J. and Mertig, Phys. Rev. Lett. **117**, 157204 (2016).
- [16] Ying Su, X. S. Wang, X. R. Wang, arXiv:1609.01500 (2016).
- [17] S. A. Owerre, arXiv:1608.00545 (2016).
- [18] C. Kane and T. C. Lubensky, Nat. Phys. **10**, 39 (2014).
- [19] B. G. Chen, N. Upadhyaya, and V. Vitelli, Proc. Natl. Acad. Sci. U.S.A. **111**, 13004 (2014).
- [20] J. Paulose, B. G. Chen, and V. Vitelli, Nat. Phys. **11**, 153 (2015).
- [21] J. Paulose, A. S. Meeussen, and V. Vitelli, Proc. Natl. Acad. Sci. U.S.A. **112**, 7639 (2015).
- [22] D. Zeb Rocklin, B. Gin-ge Chen, M. Falk, V. Vitelli, and T. C. Lubensky, Phys. Rev. Lett. **116**, 135503 (2016).
- [23] Olaf Stenull, C. L. Kane, and T. C. Lubensky, Phys. Rev. Lett. **117**, 068001 (2016).
- [24] I. Dzyaloshinsky, J. Phys. Chem. Solids **4**, 241 (1958).
- [25] T. Moriya, Phys. Rev. **120**, 91 (1960).
- [26] H.-M. Guo and M. Franz, Phys. Rev. B **80**, 113102 (2009).
- [27] M. Z. Hasan and C. L. Kane, Rev. Mod. Phys. **82**, 3045 (2010).
- [28] X.-L. Qi and S.-C. Zhang, Rev. Mod. Phys. **83**, 1057 (2011).
- [29] Lucile Savary and Leon Balents, Rep. Prog. Phys. **80**, 016502 (2017).
- [30] M. Elhajal, B. Canals, and C. Lacroix, Phys. Rev. B **66**, 014422 (2002).
- [31] O. Cépas, C. M. Fong, P. W. Leung, and C. Lhuillier Phys. Rev. B **78**, 140405(R) (2008).
- [32] D. Grohol, K. Matan, J.H. Cho, S.-H. Lee, J.W. Lynn, D.G. Nocera, Y.S. Lee, Nature Materials **4**, 323 (2005).
- [33] K. Matan, D. Grohol, D. G. Nocera, T. Yildirim, A. B. Harris, S. H. Lee, S. E. Nagler, and Y. S. Lee, Phys. Rev.

- Lett. **96**, 247201 (2006).
- [34] A. Zorko, S. Nellutla, J. van Tol, L. C. Brunel, F. Bert, F. Duc, J.-C. Trombe, M. A. de Vries, A. Harrison, and P. Mendels, Phys. Rev. Lett. **101**, 026405 (2008).
- [35] H. Yoshida, Y. Michiue, E. Takayama-Muromachi, and M. Isobe, J. Mater. Chem. **22**, 18793 (2012).
- [36] A. Zorko, F. Bert, A. Ozarowski, J. van Tol, D. Boldrin, A. S. Wills, and P. Mendels, Phys. Rev. B **88**, 144419 (2013).
- [37] A. B. Harris, C. Kallin, and A. J. Berlinsky, Phys. Rev. B **45**, 2899 (1992).
- [38] Supplemental material (<https://arxiv.org/abs/1609.03563>).
- [39] S. A. Owerre, A. A. Burkov, and Roger G. Melko, Phys. Rev. B **93**, 144402 (2016).
- [40] Steve M. Young and Charles L. Kane, Phys. Rev. Lett. **115**, 126803 (2015).
- [41] Y. Taguchi, Y. Oohara, H. Yoshizawa, N. Nagaosa, Y. Tokura, Science **291**, 2573 (2001).
- [42] Y. Machida, S. Nakatsuji, Y. Maeno, T. Tayama, T. Sakakibara, and S. Onoda, Phys. Rev. Lett. **98**, 057203 (2007).
- [43] Y. Machida, S. Nakatsuji, S. Onoda, T. Tayama, and T. Sakakibara, Nature, **463**, 210 (2008).
- [44] C. Sürgers, G. Fischer, P. Winkel and H. v. Löhneysen, Nature Commun. **5**, 3400 (2014).
- [45] Jian Zhou, Qi-Feng Liang, Hongming Weng, Y. B. Chen, Shu-Hua Yao, Yan-Feng Chen, Jinming Dong, and Guang-Yu Guo, Phys. Rev. Lett. **116**, 256601 (2016).
- [46] Luuk J. P. Ament, Michel van Veenendaal, Thomas P. Devereaux, John P. Hill, and Jeroen van den Brink, Rev. Mod. Phys. **83**, 705 (2011).
- [47] Khalil Zakeri, Physics Reports **545**, 47 (2014).
- [48] D. Watanabe, K. Sugii, M. Shimozawa, Y. Suzuki, T. Yajima, H. Ishikawa, Z. Hiroi, T. Shibauchi, Y. Matsuda, M. Yamashita, Proc. Natl. Acad. Sci. USA **113**, 8653 (2016).